

See discussions, stats, and author profiles for this publication at: <https://www.researchgate.net/publication/6666631>

# Radical/Ion Pair Formation in the Electrochemical Reduction of Arene Sulfenyl Chlorides

ARTICLE *in* JOURNAL OF THE AMERICAN CHEMICAL SOCIETY · APRIL 2007

Impact Factor: 12.11 · DOI: 10.1021/ja062796t · Source: PubMed

---

CITATIONS

19

---

READS

59

## 4 AUTHORS, INCLUDING:



Chang Ji

Texas State University

28 PUBLICATIONS 277 CITATIONS

SEE PROFILE



Mohamed Ahmida, PhD, P.Chem

Delphi

22 PUBLICATIONS 61 CITATIONS

SEE PROFILE

## Radical/Ion Pair Formation in the Electrochemical Reduction of Arene Sulfenyl Chlorides

Chang Ji, Mohamed Ahmida, M'hamed Chahma, and Abdelaziz Houmam\*

Contribution from the Electrochemical Technology Center, Department of Chemistry, University of Guelph, Guelph, Ontario, Canada N1G 2W1

Received April 28, 2006; E-mail: houmam@chembio.uoguelph.ca

**Abstract:** Important aspects of the electrochemical reduction of a series of substituted arene sulfenyl chlorides are investigated. A striking change is observed in the reductive cleavage mechanism as a function of the substituent on the aryl ring of the arene sulfenyl chloride. With *p*-substituted phenyl chlorides a "sticky" dissociative ET mechanism takes place where a concerted ET mechanism leads to the formation of a radical/anion cluster before decomposition. With *o*-nitrophenyl sulfenyl substituted chlorides a stepwise mechanism is observed where through space S...O interactions play an important role stabilizing both the neutral molecules and their reduced forms. Disulfides are generated through a nucleophilic reaction of the two-electron reduction produced anion (arenethiolate) on the parent molecule. The dissociative electron transfer theory, as well as its extension to the case of strong in-cage interactions between the produced fragments, along with the gas phase chemical quantum calculations results helped rationalize both the observed change in the ET mechanism and the occurrence of the "sticky dissociative" ET mechanism. The radical/anion pair interactions have been determined both in solution as well as in gas phase. This study shows that despite the low magnitude of in-cage interactions in acetonitrile as compared to in the gas phase, their existence strongly affects the kinetics of the involved reactions. It also shows that, as expected, these interactions are reinforced by the existence of strong electron-withdrawing substituents.

### Introduction

Particular interest has been given to the dissociative electron transfer (ET),<sup>1</sup> where a chemical bond is broken as a result of an ET to an organic or bioorganic molecule, to understand its occurrence and the factors that control it. The mechanism can either be concerted, where the ET and the bond breaking are simultaneous, or stepwise, where the ET and the bond cleavage are successive steps.<sup>2</sup> For a stepwise mechanism, the Hush–Marcus model,<sup>3</sup> of outersphere electron transfer, can be applied to the electron-transfer step. On the other hand, when the ET and the bond breaking occur in a concerted manner, a model based on the Morse curve picture of bond breaking is used.<sup>2</sup> For both mechanisms, the reaction activation energy depends on both thermodynamic and kinetic factors, through a quadratic activation-driving force relationship. The only difference being

the contribution, for a concerted ET mechanism, of the bond dissociation energy ( $D_R$ ) of the fragmented bond to the activation barrier,  $\Delta G_0^\ddagger$ , which involves only the solvent ( $\lambda_0$ ) and the inner ( $\lambda_i$ ) reorganization energies for a stepwise mechanism.

$$\Delta G_{0,s}^\ddagger = \frac{\lambda_i + \lambda_0}{4} \text{ and } \Delta G_{0,c}^\ddagger = \frac{\lambda_0 + D_R}{4} \quad (1)$$

$\Delta G_{0,s}^\ddagger$  and  $\Delta G_{0,c}^\ddagger$  (i.e., the activation energy at zero driving force) represent the intrinsic barriers for a stepwise and a concerted ET, respectively.

For a concerted mechanism, the activation free energy,  $\Delta G^\ddagger$ , is related to the driving force,  $\Delta G^\circ$ , through eq 2.

$$\Delta G^\ddagger = \frac{D_R + \lambda_0}{4} \left( 1 + \frac{\Delta G^\circ}{D_R + \lambda_0} \right)^2 \quad (2)$$

The difference in the reaction free energy between the two ET mechanisms can be expressed by the corresponding standard potentials (eq 3).

$$E_{RX/RX^\bullet}^0 - E_{RX^\bullet/RX}^0 = E_{RX/RX^\bullet}^0 + D_{R-X} - E_{X^\bullet/X}^0 - T\Delta S_{RX/RX^\bullet+X^\bullet} \quad (3)$$

The weaker the bond is and the more positive  $E_{X^\bullet/X}^0$  is, the more favorable the thermodynamics of the concerted mechanism are.

In cyclic voltammetry (CV) the peak characteristics can be used efficiently to obtain accurate mechanistic, kinetic, and

- (1) (a) Savéant, J.-M. *J. Am. Chem. Soc.* **1987**, *109*, 6788. (b) Savéant, J.-M. *Acc. Chem. Res.* **1993**, *26*, 455. (c) Savéant, J.-M. Dissociative Electron Transfer. In *Advances in Electron-Transfer Chemistry*; Mariano, P. S., Ed.; JAI Press: New York, 1994; Vol. 4, p 53–116.
- (2) For a review, see for example (a) Savéant, J.-M.; *Electron Transfer, Bond Breaking and Bond Formation*. In *Advances in Physical Organic Chemistry*; Tidwell, T. T., Ed.; Academic Press: New York, 2000; Vol. 35, pp 177–192.
- (3) See, for example (a) Marcus, R. A. *J. Chem. Phys.* **1955**, *24*, 4955. (b) Marcus, R. A. *J. Chem. Phys.* **1956**, *24*, 966. (c) Marcus, R. A. *J. Chem. Phys.* **1956**, *24*, 979. (d) Hush, N. S. *J. Chem. Phys.* **1958**, *28*, 962. (e) Hush, N. S. *Trans. Faraday Soc.* **1961**, *57*, 557. (f) Marcus, R. A. *Annu. Rev. Phys. Chem.* **1964**, *15*, 155. (g) Marcus, R. A. *J. Chem. Phys.* **1965**, *43*, 679. (h) Marcus, R. A. Theory and Applications of Electron Transfers at Electrodes and in Solution. In *Special Topics in Electrochemistry*; Rock, P. A., Ed.; Elsevier: New York 1977; pp 161–179. (i) Marcus, R. A. *Faraday Discuss. Chem.* **1982**, *74*, 7. (j) Marcus, R. A.; Sutin, N. *Biochim. Biophys. Acta* **1985**, *811*, 265.

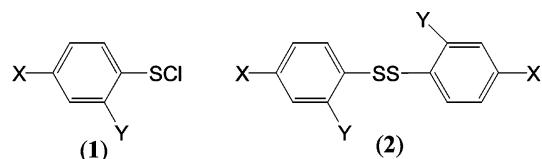
thermodynamic data by application of the adequate theory. When the single ET product cannot be detected experimentally (high scan rate<sup>4</sup> and homogeneous catalysis<sup>2,3</sup>), the transfer coefficient ( $\alpha$ ), which is directly related to the intrinsic barrier (eq 4), can be a sensitive probe of the mechanistic nature of the first electron transfer in dissociative ET processes. Experimentally, the transfer coefficient can readily be determined from the electrochemical peak characteristics (peak width,  $E_p - E_{p/2}$ ,<sup>6a</sup> or the variation of the peak potential,  $E_p$ , with the scan rate,  $v$ .<sup>6b</sup> In a concerted mechanism, a value significantly lower than 0.5 is expected, whereas an  $\alpha$  value close to or higher than 0.5 is expected in the case of a stepwise mechanism.<sup>7</sup>

$$\alpha = \frac{\partial \Delta G^\ddagger}{\partial \Delta G^0} = \frac{1}{2} \left( 1 + \frac{\Delta G^0}{4\Delta G_0^\ddagger} \right) \quad (4)$$

The dissociative ET model has been successfully tested for a number of types of organic compounds.<sup>1,2,8</sup> Equation 4 predicts a linear variation of  $\alpha$  with the driving force, however a few experimental systems have shown a nonlinear variation.<sup>9</sup> This is an indication of a transition between concerted and stepwise mechanism as a function of the driving force which could easily be controlled in electrochemistry by varying the electrode potential. This behavior demonstrates that the nature of the ET process is not dictated by the existence of an intermediate radical anion but rather by the energetic advantage of one process over another.

The dissociative ET has also been successfully used to describe the formation/dissociation reactions of radical ions.<sup>1b,2,10</sup> More recently, this theory has been extended to describe dissociative ET reactions involving strong interactions between the produced fragments ("sticky" dissociative ET).<sup>11</sup> The intermediate formation of radical/ion pairs during the concerted

Chart 1.



(a) X = CH<sub>3</sub>, Y = H; (b) X = H, Y = H; (c) X = Cl, Y = H;  
(d) X = NO<sub>2</sub>, Y = H; (e) X = H, Y = NO<sub>2</sub>; (f) X = NO<sub>2</sub>, Y = NO<sub>2</sub>

**Table 1.** Electrochemical Characteristics of Substituted Arene Sulfenyl Chlorides (**1a–f**)

ArSCl	$E_{p1}^a$ (V vs SCE)	slope <sup>b</sup> $E_p - \log(v)$	$\alpha^c$	$E_p - E_{p/2}^a$ (V)	$\alpha^d$	$E_{p2}^a$ (V vs SCE)
<b>1a</b>	−0.18	−0.121	0.25	−0.147	0.32	−1.65
<b>1b</b>	−0.21	−0.094	0.32	−0.147	0.32	−1.50
<b>1c</b>	−0.22	−0.112	0.27	−0.138	0.34	−1.47
<b>1d</b>	−0.05	−0.084	0.35	−0.138	0.34	−0.80
<b>1e</b>	−0.46	−0.054	0.54	−0.092	0.51	−0.96
<b>1f</b>	−0.27	−0.047	0.62	−0.073	0.64	−0.58

<sup>a</sup> At  $v = 200$  mV/s. <sup>b</sup> In V/unit  $\log(v)$ . <sup>c</sup> From  $E_p - \log(v)$  plot. <sup>d</sup> From peak width.

reductive cleavage of carbon tetrachloride,<sup>11a,b</sup> 4-cyanobenzyl chloride,<sup>11b</sup> haloacetonitriles,<sup>11c</sup> and polychloroacetamides<sup>11d</sup> has been shown to affect both the mechanism and the rate of these ET processes. More recently, the existence of such in-cage interactions during the electrochemical reduction of substituted benzyl thiocyanates<sup>12</sup> has been shown to affect the regioselective bond cleavage and hence the outcome of the chemical reaction through the dissociation of a chemical bond that seems otherwise very stable. The strength of these interactions has been shown to depend on the Lewis acid–base properties of the involved fragments as well as on the nature of the used solvent as expected.<sup>11</sup> In these studies, it has been demonstrated that, despite the fact that their magnitude is smaller in polar solvents compared to that in gas phase, these in-cage interactions strongly affect the dissociative ET processes to the latter molecules. A new activation free energy–standard free energy quadratic relationship, involving the contribution of the interaction energy in the radical-ion pair ( $D_P$ ) has been obtained when extending the dissociative ET to the case of radical-ion pair formation (eq 5).<sup>11</sup> The accuracy of this model has been demonstrated through its application to heterogeneous<sup>11</sup> as well as homogeneous<sup>9b,13</sup> ET reactions. Additional experimental examples involving the intermediate formation of such radical-ion pairs ( $\sigma$  radical ions) would provide more insights into the factors controlling such phenomenon as well as into its consequences on the chemical reactions.

$$\Delta G^\ddagger = \frac{(\sqrt{D_R} - \sqrt{D_P})^2 + \lambda_0}{4} \left( 1 + \frac{\Delta G^0 - D_P}{(\sqrt{D_R} - \sqrt{D_P})^2 + \lambda_0} \right)^2 \quad (5)$$

Sulfenyl chlorides and their derivatives are of great importance because of their high reactivity, versatile chemistry, and

- (4) (a) Andrieux, C. P.; Hapiot, P.; Savéant, J.-M. *Chem. Rev.* **1990**, *90*, 723. (b) Andrieux, C. P.; Hapiot, P.; Savéant, J.-M. *J. Phys. Chem.* **1988**, *92*, 5987.  
(5) Andrieux, C. P.; Savéant, J.-M. *Electrochemical Reactions. In Investigation of Rates and Mechanisms of Reactions, Techniques of Chemistry*; Bernasconi, C. F., Ed.; Wiley: New York, 1986; Vol. VI/4E, Part 2, pp 305–390.  
(6) (a)  $\alpha = (RT/F)(1.85/E_{p/2} - E_p)$ . (b)  $\partial E_p/\partial \log v = -29.5/\alpha$  at 20°C.  
(7) Cases have been encountered where an important internal intrinsic barrier is associated with a stepwise ET and in certain cases a low transfer coefficient: (a) Severin, M. G.; Avéralo, M. C.; Maran, F.; Vianello, E. *J. Phys. Chem.* **1993**, *97*, 150. (b) Jakobson, S.; Jensen, H.; Pederson, S. U.; Daasbjerg, K. *J. Phys. Chem. A* **1999**, *103*, 4141. (c) Christensen, T. B. Daasbjerg, K. *Acta Chem. Scand.* **1997**, *51*, 307. (d) Daasbjerg, K.; Jensen, H.; Benassi, R.; Taddei, F.; Antonello, S.; Gennaro, A.; Maran, F. *J. Am. Chem. Soc.* **1999**, *121*, 1750. (e) Maran, F.; Benassi, R.; Gavioli, G.; Taddei, F.; Maran, F. *J. Am. Chem. Soc.* **2002**, *124*, 7529. (f) Antonello, S.; Daasbjerg, K.; Jensen, H.; Taddei, F.; Maran, F. *J. Am. Chem. Soc.* **2003**, *125*, 14905. (g) Isse, A. A.; Gennaro, A.; Maran, F. *Acta Chem. Scand.* **1999**, *53*, 1013.  
(8) See for examples (a) Savéant, J.-M. *Adv. Phys. Org. Chem.* **1990**, *26*, 1. (b) Andrieux, C. P.; Le Gorand, A.; Savéant, J.-M. *J. Am. Chem. Soc.* **1992**, *112*, 6892. (c) Savéant, J.-M. *J. Am. Chem. Soc.* **1992**, *114*, 10595. (d) Bertran, J.; Gallardo, I.; Moreno, M.; Savéant, J.-M. *J. Am. Chem. Soc.* **1992**, *114*, 9576. (e) Adcock, W.; Clark, C.; Houmam, A.; Krstic, A. R.; Pinson, J.; Savéant, J.-M.; Taylor, D. K.; Taylor, J. F. *J. Am. Chem. Soc.* **1994**, *116*, 4653.  
(9) (a) Houmam, A.; Hamed, E. M.; Still, I. W. *J. Am. Chem. Soc.* **2003**, *125*, 7258. (b) Costentin, C.; Hapiot, P.; Médebielle, M.; Savéant, J.-M. *J. Am. Chem. Soc.* **2000**, *122*, 5623. (c) Pause, L.; Robert, M.; Savéant, J.-M. *J. Am. Chem. Soc.* **2001**, *123*, 4886. (d) Andrieux, C. P.; Robert, M.; Saeva, F. D.; Savéant, J.-M. *J. Am. Chem. Soc.* **1994**, *116*, 7864. (e) Pause, L.; Robert, M.; Savéant, J.-M. *J. Am. Chem. Soc.* **1999**, *121*, 7158. (f) Antonello, S.; Maran, F. *J. Am. Chem. Soc.* **1997**, *119*, 12595. (g) Andrieux, C. P.; Savéant, J.-M. *J. Electroanal. Chem.* **1986**, *205*, 43.  
(10) (a) Savéant, J.-M. *J. Phys. Chem.* **1994**, *98*, 3716. (b) Laage, D.; Burghardt, I.; Sommerfeld, T.; Hynes, J. T. *J. Phys. Chem. A* **2003**, *107*, 11292. (c) Burghardt, I.; Laage, D.; Hynes, J. T. *J. Phys. Chem. A* **2003**, *107*, 11271. (d) Costentin, C.; Robert, M.; Savéant, J.-M. *J. Am. Chem. Soc.* **2004**, *106*, 16051.  
(11) (a) Pause, L.; Robert, M. Savéant, J.-M. *J. Am. Chem. Soc.* **2000**, *122*, 9829. (b) Pause, L.; Robert, M. Savéant, J.-M. *J. Am. Chem. Soc.* **2001**, *123*, 11908. (c) Cardinale, A.; Isse, A. A.; Gennaro, A.; Robert, M.; Savéant, J.-M. *J. Am. Chem. Soc.* **2002**, *124*, 13533. (d) Costentin, C.; Louault, C.; Robert, M.; Teillout, A.-L. *J. Phys. Chem. A* **2005**, *109*, 2984. (e) Savéant, J.-M. *J. Phys. Chem. B* **2001**, *105*, 8995.  
(12) Hamed, E. M.; Doai, H.; McLaughlin, C. K.; Houmam, A. *J. Am. Chem. Soc.* **2006**, *128*, 6595.  
(13) Isse, A. A.; Gennaro, A. *J. Phys. Chem. A* **2004**, *108*, 4180.

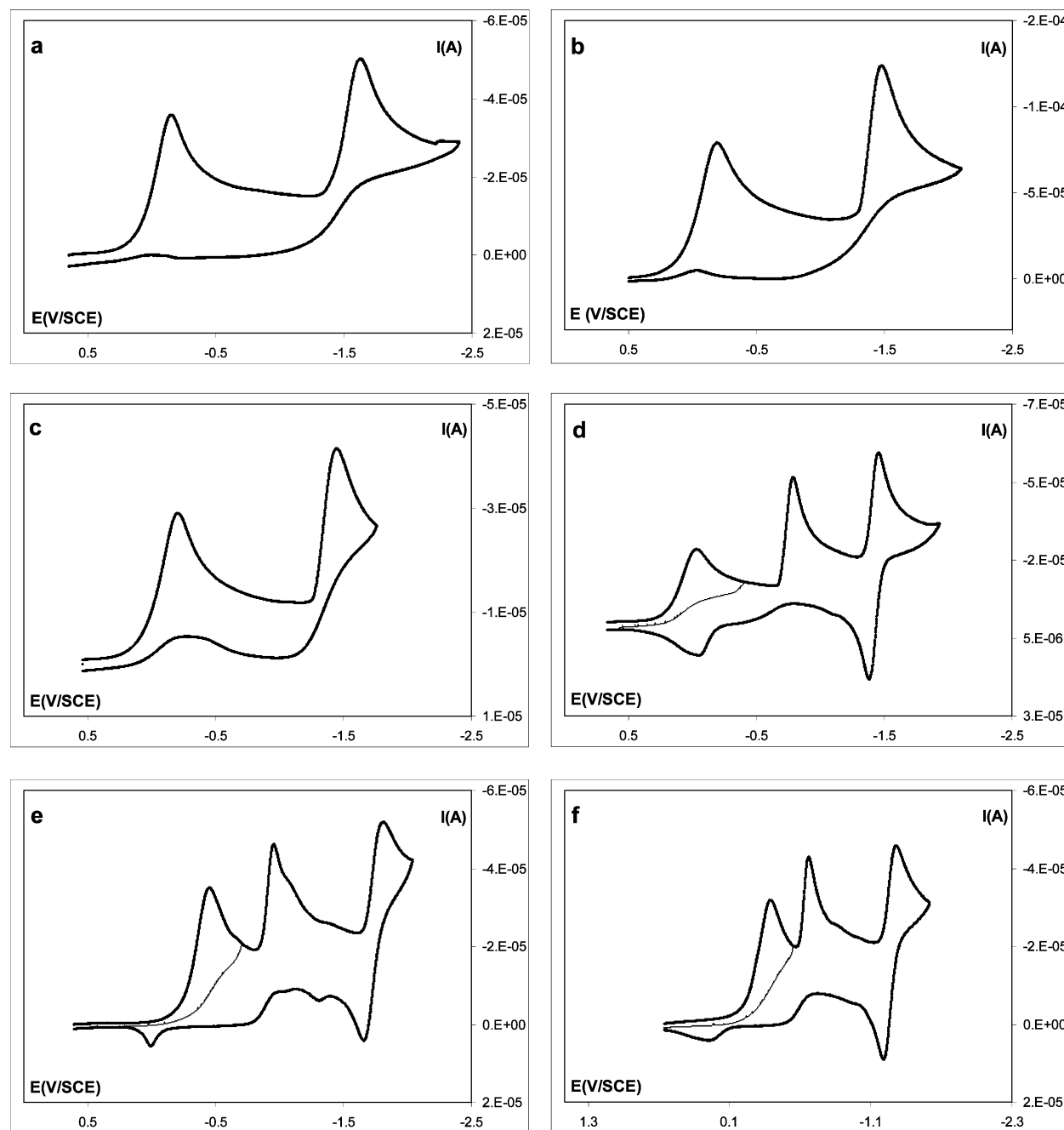


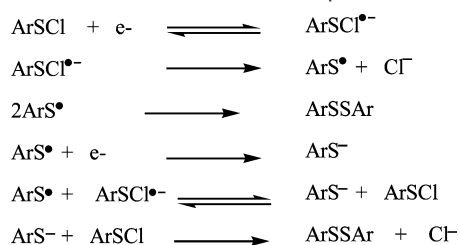
**Figure 1.** Cyclic voltammetry in  $\text{CH}_3\text{CN}/\text{NBu}_4\text{PF}_6$  (0.1 M) at a glassy carbon electrode at  $v = 200$  mV/s of (a) **1a** (2.65 mM), (b) **1b** (2.16 mM), (c) **1c** (2.18 mM), (d) **1d** (1.90 mM), (e) **1e** (2.12 mM), and (f) **1f** (2.10 mM).

wide range of applications.<sup>14</sup> We are particularly interested in investigating the dynamics of their reduction through a careful analysis of the involved mechanisms as well as a rigorous determination of the factors controlling their kinetics and thermodynamics. We previously reported the electrochemistry of the 2- and 4-nitroarene sulfonyl chlorides and showed that their reduction results in the cleavage of the S–Cl bond.<sup>15</sup> Our initial investigation showed that while the electrochemical reduction of 2-nitroarene sulfonyl chloride follows a step-wise ET mechanism that of the 4-nitroarene sulfonyl chloride follows probably a sticky dissociative ET mechanism involving the formation of a radical/anion (4-nitrophenyl

sulfonyl/chloride) pair. This manuscript describes the full investigation of a more extended series of substituted benzyl sulfonyl chlorides **1a–f** (Chart 1). Not only is a change of the ET mechanism observed but more interestingly, a clear-cut example of a sticky dissociative ET is encountered. The factors controlling the ET mechanism variation as well as the extent of the in-cage interactions between the reduction fragments are discussed on the basis of the dissociative ET theory and its extension to the case of in-cage interactions (sticky dissociative ET).<sup>11,12</sup> Theoretical calculations help rationalize both the difference in the ET mechanism as well as the cluster formation.

(14) See for example: Abu-Yousef, I. A.; Harpp, D. N. *Sulfur Rep.* **2003**, *24*, 255.

(15) Ji, C.; Goddard, J. D.; Houmam, A. *J. Am. Chem. Soc.* **2004**, *126*, 8076.

**Scheme 1.** Reduction Mechanism for Compounds **1e,f**

## Results and Discussion

**Voltammetric Behavior.** The electrochemical reduction of substituted arene sulfonyl chlorides (**1a–f**) and their corresponding disulfides (**2a–f**) was studied by cyclic voltammetry (CV) in acetonitrile, in the presence of tetrabutylammonium hexafluorophosphate (TBAH 0.1 M) at a glassy carbon electrode. The peak characteristics (peak potential ( $E_p$ ), peak width ( $E_p - E_{p/2}$ ), slope ( $E_p - \log(\nu)$ ) and transfer coefficient ( $\alpha$ ) values determined from both peak width and  $E_p - \log(\nu)$  plots) are summarized in Table 1.

Figure 1a shows a cyclic voltammogram that corresponds to 4-methylphenyl sulfonyl chloride (**1a**). It displays a first cathodic peak ( $E_p = -0.18$  V versus SCE), corresponding to the irreversible reduction of **1a** (Figure 1a). Its height, measured by reference to the monoelectronic wave of ferrocene, corresponds to the consumption of one electron per molecule. The transfer coefficient values determined from both the first reduction peak width<sup>6a</sup> and from the  $E_p - \log(\nu)$  plot<sup>6b</sup> correspond to 0.31 and 0.33, respectively, that is, much lower than 0.5 indicating a reaction kinetically controlled by the electron-transfer step.<sup>1,2</sup> The second irreversible peak at  $E_p = -1.44$  V versus SCE corresponds to the reduction peak of bis-(4-methylphenyl) disulfide (**2a**) by comparison with an authentic sample. Compounds **1a–d** show similar characteristics for the first reduction peak as they all present an initial broad peak with low  $\alpha$  values (0.25–0.35) and a peak height corresponding to the consumption of one electron per molecule. Compound **1d** shows a third reduction peak at  $E = -1.42$  V versus SCE corresponding to the second reduction peak of bis(4-dinitrophenyl) disulfide (**4d**).

Compounds **1e,f** show similar electrochemical characteristics. Figure 1e shows the cyclic voltammogram of 2-nitrobenzenesulfonyl chloride (**1e**), which displays a first monoelectronic irreversible reduction peak at a potential  $E_p = -0.46$  V versus SCE, 420 mV more negative than **1d**. This is an unexpectedly large difference. For comparison, in the benzyl bromides the difference between the reduction potentials of the *p*- and *o*-nitro substrates is only 8 mV.<sup>8b</sup> The first peak width has a value of 92 mV and the slope of the  $E_p - \log(\nu)$  plot is equal to  $-55$  mV per unit  $\log(\nu)$ . These peak characteristics (Table 1) correspond to a stepwise ET involving the intermediacy of a radical anion and with a mixed kinetic control by both the ET and the bond dissociation steps (Scheme 1).<sup>1,2</sup> The first peak is followed by a second irreversible peak ( $E_p = -0.96$  V versus SCE) and a third reversible peak at  $E^\circ = -1.74$  V versus SCE corresponding, respectively, to the first and second reduction peaks of bis(2-nitrophenyl) disulfide (**2e**), by comparison with an authentic sample.<sup>16</sup> Compound **1f** shows a similar behavior compared to **1e**. The first reduction peak ( $E_p = -0.27$  V versus SCE) is narrow, with a peak width value of 73 mV, and a low

**Table 2.** Electrolyses Results of Substituted Arene Sulfonyl Chlorides (**1a–f**)

ArSCl	ArSSAr (%)	ArSO <sub>2</sub> SAr (%)
<b>1a</b>	81	18
<b>1b</b>	83	17
<b>1c</b>	79	17
<b>1d</b>	85 <sup>a</sup>	12
<b>1e</b>	95 <sup>a</sup>	
<b>1f</b>	95 <sup>a</sup>	

<sup>a</sup> Small amounts of the thiolate anion which did not react were also detected.

slope value for the  $E_p - \log(\nu)$  plot ( $-47$  mV/ $\log(\nu)$ ). Similarly, a second irreversible peak ( $E_p = -0.58$  V versus SCE) and a third reversible wave ( $E^\circ = -1.27$  V versus SCE) are observed corresponding, respectively, to the first and second reduction of the bis(2,4-dinitrophenyl) disulfide (**2f**), by comparison with an authentic sample. All nitro compounds **1d–f** show a forth reduction peak corresponding to the reduction of the nitro group at more negative potentials.

An intriguing first observation is that the reduction potentials of **1e,f** are more negative than those corresponding to **1a–d** despite the presence of nitro groups. We previously suggested that, for compounds **1d** and **1e**, this difference is mainly due to the through space S $\cdots$ O interaction in **1e** because of the proximity of the nitro group.<sup>15</sup> Further evidence for the existence of such through space interaction will be provided through the investigation of compound **1f**. Moreover, the nature of the involved initial ET mechanism is also another important factor as will be demonstrated in this manuscript.

Electrolyses of compounds **1a–f** have been performed in acetonitrile, in the presence of tetramethylammonium tetrafluoroborate (0.1 M), and the results of all studied compounds **1a–f** are reported in Table 2. The main product for all compounds is the corresponding disulfide (**2a–f**). For compounds **1a–d**, considerable quantities of the corresponding thiosulfonates (ArSO<sub>2</sub>SAr) are obtained. These compounds are yielded through a well-known chemical process through the intermediate formation of the corresponding aryl thiosulfinate (ArS(O)SAr).<sup>17</sup> A control reaction has been performed where chlorine has been added to **1a–d** and the reaction yielded the corresponding disulfides (**2a–d**) and thiosulfonates. In fact, the determined number of electrons consumed during the electrolyses of compounds **1a–d** is lower than 1. Compounds **1e,f** yield the corresponding disulfides quantitatively after the consumption of one electron per molecule.

To gain more insights into the understanding of the initial ET nature, a theoretical study at the B3LYP level of the substituted arene sulfonyl chlorides (**1a–f**) and their corresponding reduced forms has been performed.

- (16) (a) The disulfides are generated as for the thiocyanates.<sup>16b,c</sup> The nitrophenyl radical resulting from the initial ET is reduced at the electrode to yield the corresponding thiolate anion.<sup>16d</sup> The yielded thiolate attacks the initial sulphenyl chloride to generate the corresponding disulfide. (b) Houmam, A.; Hamed, E. M.; Still, I. W. *J. Am. Chem. Soc.* **2003**, *125*, 7258. (c) Houmam, A.; Hamed, E. M.; Hapiot, P.; Motto, J. M.; Shwan, A. L. *J. Am. Chem. Soc.* **2003**, *125*, 12676. (d) The standard reduction potentials of the some substituted phenyl thiolates have been determined.<sup>16e,f</sup> (e) Andreux, C. P.; Hapiot, P.; Pinson, J.; Savéant, J.-M. *J. Am. Chem. Soc.* **1993**, *115*, 7783. (f) Larsen, A. G.; Holm, A. H.; Roberson, M.; Daasbjerg, K. *J. Am. Chem. Soc.* **2001**, *123*, 1723. (g) The standard oxidation potentials of the other substituted aryl thiolates can be deduced using data in ref 16e,f.
- (17) Bontempelli, G.; Magno, F.; Seeber, R.; Mazzocchin, G. A. *J. Electroanal. Chem.* **1978**, *87*, 73.



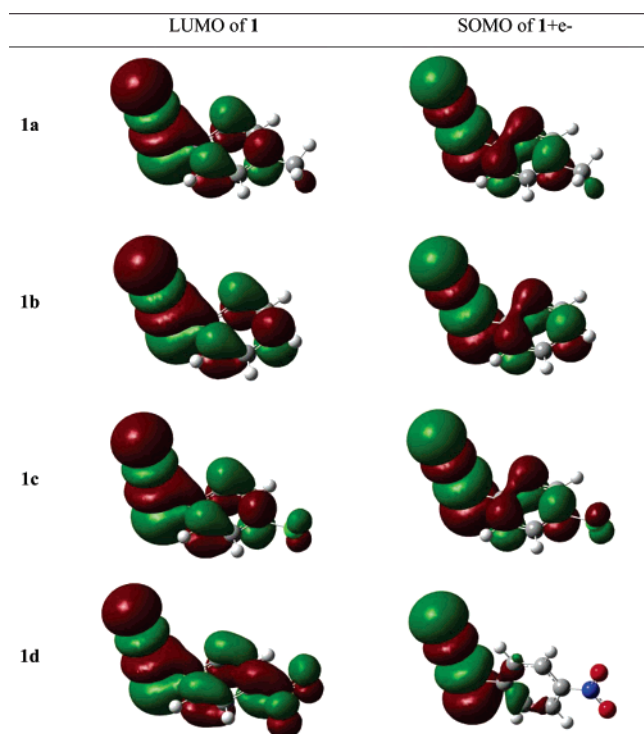


**Figure 2.** LUMOs and SOMOs of **1a–d** and their reduced forms, respectively.

**Theoretical Study.** Figures 2 and 3 show the LUMOs of compounds **1a–f** and the SOMOs of their corresponding reduced forms (radical anions or radical/anion pairs)<sup>11–13</sup> and a series of observations can be made.

Figure 2 shows that for compounds **1a–d**, the LUMOs are more located on the S–Cl group with a lower factor on the aryl moiety, hence increasing the probability of injecting the extra electron directly into the  $\sigma$  S–Cl bond leading to its dissociation. The SOMOs corresponding to their reduced forms clearly support this idea as they are more localized on the S–Cl group ( $\sigma$  radical anion or radical/ion pair). It is worth noting that the reduced forms show the S–Cl distance between 2.79 and 2.86 Å (Table 3) indicating that these reduced forms are not true radical anions but rather radical/ion pairs. This is a further support for the electrochemical data, which indicate the implication of a concerted reduction process and not a stepwise one. This will be further investigated later.

**Table 3.** S–Cl Bond Dissociation Energy and Bond Length for **1a–f** before and after Reduction

	1a	1b	1c	1d	1e	1f
$D_{S-Cl}^a$	40.13	40.45	39.97	47.65	53.29	53.83
$d_{S-Cl}(\mathbf{1})^b$	2.12	2.11	2.11	2.10	2.13	2.12
$d_{S-Cl}(\mathbf{1} + e^-)^b$	2.86	2.85	2.83	2.79	2.45	2.42
$\Delta d_{S-Cl}^b$	0.74	0.74	0.72	0.69	0.32	0.30

<sup>a</sup> Bond dissociation energy in kcal/mol. <sup>b</sup> bond length in Å.

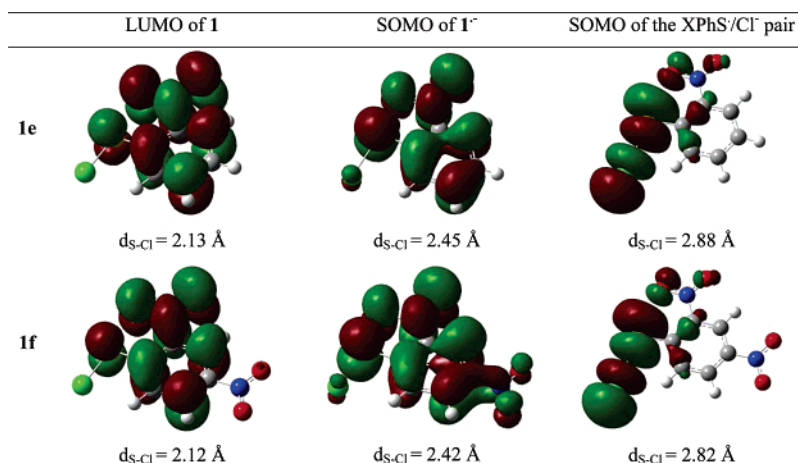
**Table 4.** S···O Distances for **1e,f** and Their Radical Anions<sup>a</sup>

	1e	1f
$d_{S\cdots O}(\mathbf{1})$ (Å)	2.34	2.36
$d_{S\cdots O}(\mathbf{1}^{\bullet-})$ (Å)	1.95	1.96

<sup>a</sup> Determined from the theoretical calculations.

For compounds **1e,f** (Figure 3), the LUMOs are more delocalized over the nitro-substituted aryl moiety indicating the incoming electron would be injected into the  $\pi^*$  yielding a radical anion intermediate. For these compounds, radical anions (**1e,f**<sup>•−</sup>) are in fact obtained and their SOMOs also delocalized over the nitro-substituted aryl moieties as seen on Figure 3. These radical anions are observed at S–Cl distances shorter than the ones observed for the reduced forms of compounds **1a–d** (Table 3). Interestingly another minimum is obtained for the reduced form for each of these compounds. These minima are observed at S–Cl bond distances similar to those observed for the reduced forms of compounds **1a–d** and larger than for the radical anions **1e,f**<sup>•−</sup>. It is worth noting that for these intermediates the electron density is totally located on the S–Cl bond. This indicates that the radical anions **1e,f**<sup>•−</sup>, formed through a stepwise ET mechanism upon reduction of compounds **1e,f**, most likely yield the corresponding radical/ion pairs before falling apart.

Table 3 shows the difference in the S–Cl bond distance as a result of the injection of an extra electron. While the S–Cl bond distance increases by only 0.32 Å and no structural changes are observed for **1e,f** upon injecting an electron, the S–Cl bond distance increase is much larger for compounds **1a–d** ( $\geq 0.70$  Å) and, for compound **1d**, is associated with an important rotation of the C–S bond upon going from the nonplanar neutral molecule to its reduced form. This indicates that while the reduction of **1e,f** leads to a radical anion through a stepwise ET mechanism (Scheme 1), that of compounds **1a–d** leads rather to a radical/anion pair through a sticky dissociative ET

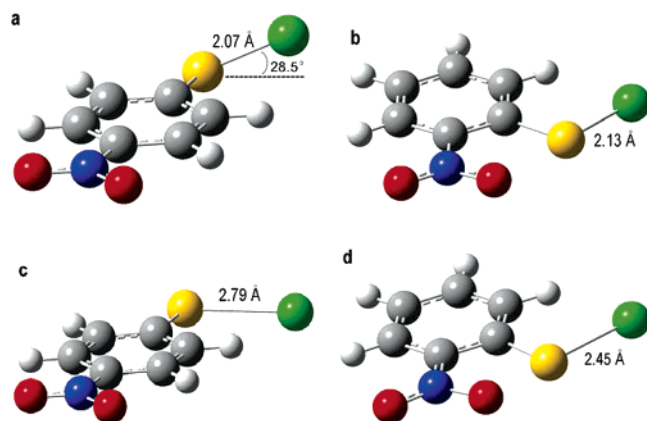


**Figure 3.** LUMOs and SOMOs of **1e,f** and their reduced forms, respectively.

**Table 5.** Parameters for Arene Sulfenyl Chlorides **1a–d**

1	$\Delta S^0$ <sup>a</sup> , $T\Delta S^0$ <sup>b</sup>	$E_{\text{Cl}^-/\text{Cl}}^0$ <sup>c</sup>	$E^0$ <sup>d</sup>	$a_{\text{Cl}}^e$	$a_{\text{ArSCl}}^e$	$a^e$	$D^f$	$Z^g$	$\lambda_0^h$
<b>1a</b>	30.45; 0.392	1.86	0.511	1.81	4.62	2.91	$2.6 \times 10^5$	4980	1.03
<b>1b</b>	27.62; 0.349	1.86	0.462	1.81	4.48	2.38	$2.7 \times 10^5$	5217	1.04
<b>1c</b>	27.64; 0.349	1.86	0.483	1.81	4.59	2.90	$2.8 \times 10^5$	4692	1.03
<b>1d</b>	27.31; 0.345	1.86	0.148	1.81	4.60	2.90	$2.8 \times 10^5$	4552	1.04

<sup>a</sup> In cal/mol·K. <sup>b</sup> In eV. <sup>c</sup> In V vs SCE. <sup>d</sup>  $E^0 = E_{\text{ArSCl}/\text{ArS}^+ + \text{Cl}^-}^0$  in V vs SCE. <sup>e</sup> In Å. <sup>f</sup> In cm<sup>2</sup>/s. <sup>g</sup> In cm/s. <sup>h</sup> In eV.

**Figure 4.** Optimized geometries of (a) **1d**, (b) **1e**, (c) **1d** +  $e^-$  and (d) **1e**  $^-$ .

mechanism in agreement with the electrochemical results. The electrochemical reduction mechanism for compounds **1e,f** can then be written (Scheme 1).

The initial electron transfer leads to intermediate formation of a radical anion (**1e,f** $^-$ ), which decomposes to produce a substituted aryl thiyl radical and a chloride anion. The aryl thiyl radical can be reduced either in solution, by the parent radical anion, or at the electrode to generate the corresponding thiolate anion. This later intermediate reacts on the initial sulfenyl chloride to produce the corresponding disulfide (**2e,f**). The disulfide may also be formed through a dimerization of the aryl thiyl radical since the initial ET follows a stepwise mechanism and the radical anion can diffuse in solution and also because of the potential, not very negative, at which the reduction of **1e,f** takes place.

Another important result concerns the difference between the nitro-substituted arene sulfenyl chlorides (**1d** on one side and **1e,f** on the other). We already suggested in an earlier communication that the difference in behavior between **1d** and **1e** is due to the through space S $\cdots$ O interaction that exists for the latter compounds.<sup>15</sup> Such an interaction stabilizes the intermediate radical anion **1e** $^-$  formed during the electrochemical reduction of **1e**. This interaction exists also for **1e** but is stronger for the radical anion (**1e** $^-$ ). The optimized structures of compounds **1d** and **1e** as well as their reduced forms help understand the presence of this interaction and its extent (Figure 4) by considering the conformations of the two compounds before and after reduction. The structure of **1d**, for which such an interaction does not exist, is not planar and the S–Cl bond axis is at a 28.5° angle from the aryl moiety plane. It is worth noting that the increase of the S–Cl bond going from the neutral to the reduced form is considerable (0.72 Å). On the other hand, the structure of both **1e** and its reduced form are planar and the S–Cl bond is aligned with the  $\pi$  system. The increase of the S–Cl bond upon going from the neutral to the reduced species is only (0.32 Å) for **1e** indicating the formation of a true radical

anion. A very important parameter is the S $\cdots$ O distances, which have been regarded as indicative of an attractive interaction between these two atoms.<sup>18</sup> The distance between the oxygen and the sulfur atoms in **1e** is 2.34 Å, similar to the experimental values (Table 4).<sup>18a</sup> This distance decreases to 1.95 Å in **1e** $^-$  which is smaller than the sum of the van der Waals' radii of sulfur and oxygen (3.25 Å) indicating a strong interaction between the two atoms for the *o*-nitrophenyl sulfenyl chloride. Such a stabilizing interaction for both the neutral molecule and the corresponding radical anion is lacking for **1d**. Further support for this idea comes from the behavior of compound **1f**. Quantum chemical calculations show that the through space S $\cdots$ O interaction exists also for 2,4-dinitro phenyl sulfenyl chloride (**1f**), which is, with **1e**, the only two compounds in this series to follow a stepwise ET mechanism upon electrochemical reduction. In **1f** the S $\cdots$ O distance is only 2.36 Å and decreases for **1f** $^-$  to 1.96 Å, indicating again the existence of this attractive interaction between the two atoms and a stronger stabilization of the radical anion compared to the neutral species. This intramolecular interaction favors a stepwise mechanism through the stabilization of the radical anion for compounds **1e,f**.

If for compounds **1e,f** both electrochemical as well as theoretical data show clearly the occurrence of a stepwise electron-transfer mechanism, compounds **1a–d** need to be further investigated to better clarify the nature of the first electron transfer, that is, to see whether important interactions between the radical/anion fragments exist. To that end we undertook the task of applying both the “classical” dissociative ET model (eq 2) and the “sticky” dissociative ET (eq 5) for these compounds. Comparison of the intrinsic barrier as a function of the driving force obtained through either models with the experimental data obtained through convolution analysis<sup>19</sup> of the cyclic voltammetric data is presented.

A series of parameters need to be determined in order to apply either model. The standard potential ( $E_{\text{ArSCl}/\text{ArS}^+ + \text{Cl}^-}^0$ ) can be estimated through eq 6.

$$E_{\text{ArSCl}/\text{ArS}^+ + \text{Cl}^-}^0 = E_{\text{Cl}^-/\text{Cl}}^0 - D_{\text{ArS-Cl}} + T\Delta S^0 \quad (6)$$

The  $E_{\text{Cl}^-/\text{Cl}}^0$  (1.86 V versus SCE in CH<sub>3</sub>CN) has been estimated from its known value in water.<sup>20</sup> The bond dissociation energy-

- (18) (a) Markham, G. D.; Bock, C. W. *J. Mol. Struct.* **1997**, *418*, 139. (b) Creed, T. Leardini, R.; McNab, H.; Nanni, D.; Nicolson, I. S.; Parkin, A.; Parsons, S. *Acta Crystallogr.* **2001**, *C57*, 1174. (c) Kucsman, A.; Kapovits, I.; Czugler, M.; Párkányi, L.; Kálmán, A. *J. Mol. Struct.* **1989**, *198*, 339. (d) Párkányi, L.; Kálmán, A.; Kucsman, A.; Kapovits, I. *J. Mol. Struct.* **1989**, *198*, 355. (e) Csonka, I. P.; Vass, G.; Szepes, L.; Szabo, D.; *J. Mol. Struct. THEOCHEM* **1998**, *455*, 141. (f) Wu, S.; Greer, A. *J. Org. Chem.* **2000**, *65*, 4883. (g) Angyán, J. G.; Poirier, R. A.; Kucsman, A.; Csizmadia, I. G. *J. Am. Chem. Soc.* **1987**, *109*, 2237. (h) Garratt, D. G.; Beaulieu, P. L. *J. Org. Chem.* **1979**, *44*, 3555. (i) Beaulieu, P. L.; Kabo, A.; Garratt, D. *Can. J. Chem.* **1980**, *58*, 1014. (19) (a) Savéant, J.-M.; Tessier, D. *J. Electroanal. Chem.* **1975**, *65*, 57. (b) Savéant, J.-M. *J. Phys. Chem. B* **2002**, *106*, 9387. (20) (a) The  $E_{\text{Cl}^-/\text{Cl}}^0$  was calculated from the equation  $E_{\text{Cl}^-/\text{Cl}}^0 = E_{\text{Cl}^-/\text{Cl-H}_2\text{O}}^0 - \Delta G_{\text{Cl-H}_2\text{O} \rightarrow \text{CH}_3\text{CN}}^0$ .<sup>20b</sup> (b) Marcus, Y. *Pure Appl. Chem.* **1985**, *57*, 1105.

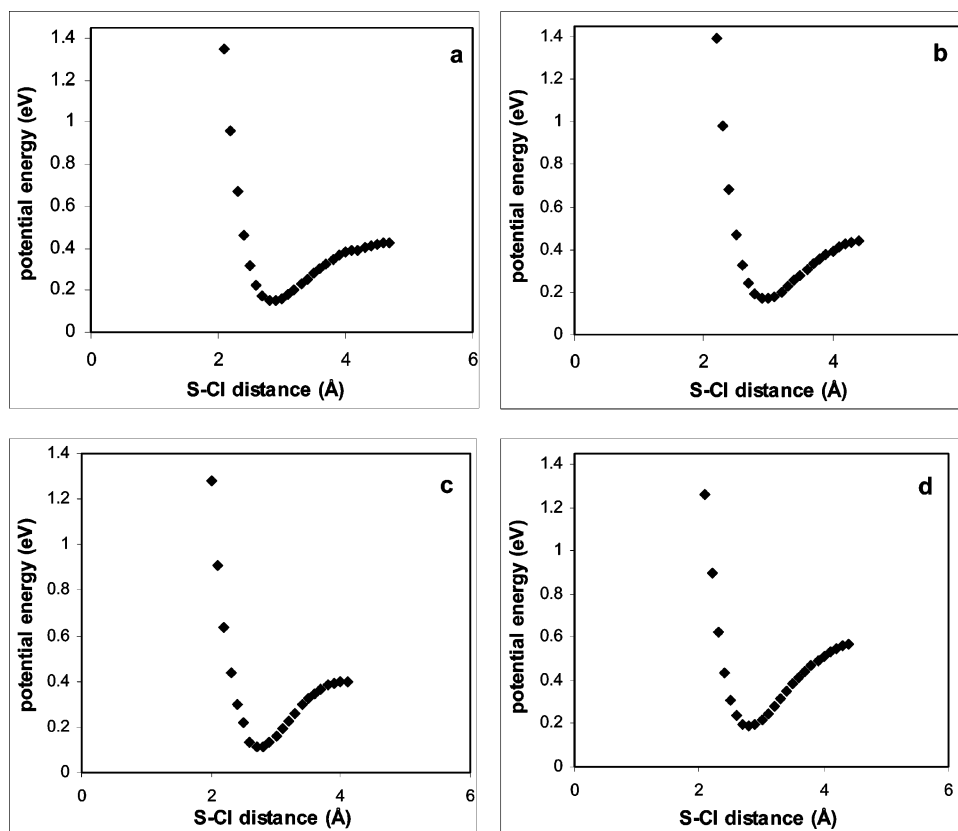


**Figure 5.** Calculated (B3LYP/6-31G(p,d)) potential energy profiles in the gas phase for the XPh/Cl<sup>−</sup> pair for (a) **1a**, (b) **1b**, (c) **1c**, and (d) **1d**.

( $D_{\text{ArS}} - \text{Cl}$ ) as well as the bond dissociation entropy ( $\Delta S^\circ$ ) of the S–Cl bond in the aryl sulfonyl chlorides were calculated.<sup>21</sup>

The solvent reorganization energies ( $\lambda_0$ ) are derived from the corresponding radii ( $a$ ) of the equivalent spheres according to eq 7.<sup>8c,22</sup>

$$\lambda_0 = 3/a \quad \text{where} \quad a = \frac{a_{\text{Cl}}(2a_{\text{ArS}} - a_{\text{Cl}})}{a_{\text{ArS}}} \quad (7)$$

The values of these parameters are listed in Table 5.

The activation free energy can also be deduced from experimental data according to eq 8.

$$\Delta G^\ddagger = \frac{RT}{F} \ln\left(\frac{Z}{k(E)}\right) \quad (8)$$

where  $k(E)$  is the potential-dependent rate constant of the electron transfer that is readily derived through convolution analysis of the cyclic voltammetric data using eq 9.

$$\ln k(E) = \ln D^{1/2} - \ln\left(\frac{I_1 - I}{i}\right) \quad (9)$$

where  $I$  is the convolutive current obtained through convolution of the CV current ( $i$ ) according to eq 10 and  $I_1$  is the limiting convolutive current  $I_1 = FSC^0D^{1/2}$ .  $S$  is the electrode surface area,  $C^0$  is the substrate concentration, and  $D$  is its diffusion coefficient.

$$I = 1/\sqrt{\pi} \int_0^t \frac{i(\eta)}{\sqrt{t - \eta}} d\eta \quad (10)$$

The preexponential factor is taken as the collision frequency

( $Z$ ) and is determined through eq 11, where  $M$  is the molar mass.

$$Z = \sqrt{RT/2\pi M} \quad (11)$$

With these parameters available, a comparison between the experimental data and the ones obtained through the use of the classical dissociative ET (eq 2) has been possible and does not lead to a good agreement. For all compounds, the predicted activation energy is larger than the experimental one. Another alternative is to use the sticky dissociative ET model (eq 3), taking into consideration a potential interaction between the radical and the anion fragments (substituted aryl radical/chloride anion) generated as a result of the initial ET. Such interaction is suggested by both our electrochemical data (reduction potentials for **1a–d** being less negative than **1e,f**) and also by the minima found for the theoretical optimization of the reduced forms of compounds **1a–d**. It has in fact been shown previously that such interaction decreases the activation energy.<sup>11</sup>

To estimate the interaction energy,  $D_p$ , and to verify the existence of fragment clustering, quantum calculations have been performed to determine the gas-phase potential energy<sup>23</sup> profile of the reduced forms of the studied compounds (**1a–d** + one electron) along the cleaved S–Cl bond. These energy profiles

(21) The BDEs have been calculated as the difference between the total molecular energy of the neutral molecules and that of the radical fragments obtained by homolytic dissociation. The entropies were also deduced as  $\Delta S^\circ = S^\circ_{\text{ArS}} - (S^\circ_{\text{ArS}^\bullet} + S^\circ_{\text{Cl}^\bullet})$ .

(22) Andrieux, C. P.; Savéant, J.-M.; Tardy, C. *J. Am. Chem. Soc.* **1998**, *1209*, 4167.

(23) What is represented on the plots in Figure 4 is not the absolute potential energy but rather the difference between the absolute value and a value lower than the minimum energy.



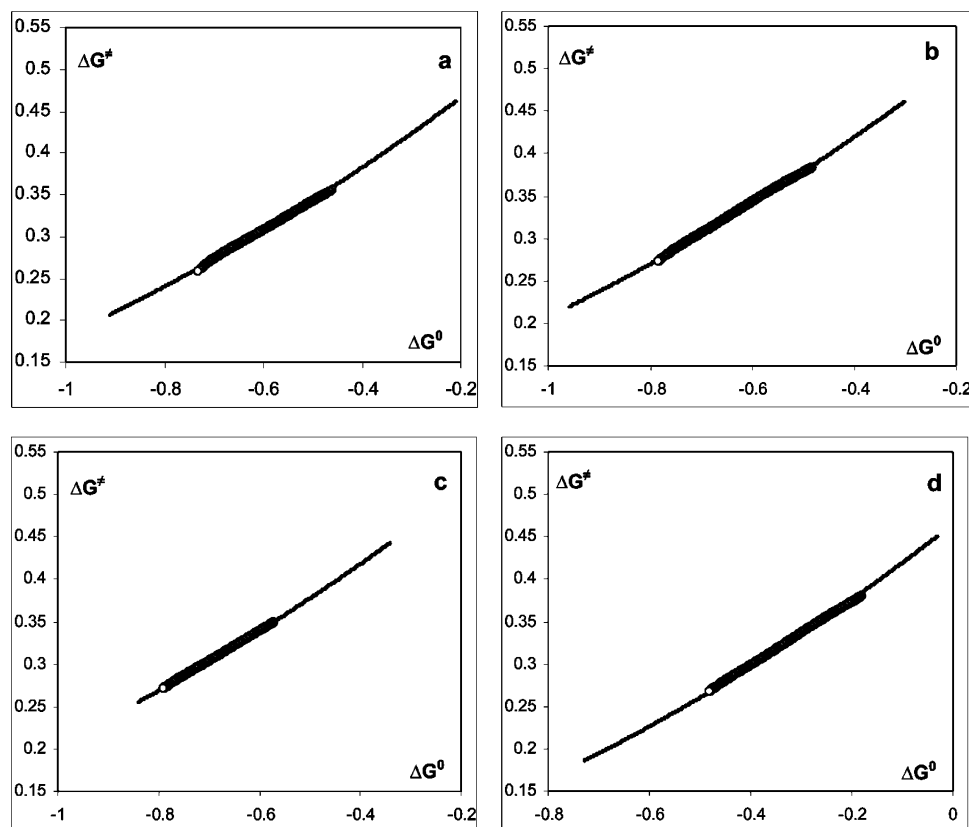


**Figure 6.** Experimental and predicted activation free energy vs standard free energy plots for (a) **1a**, (b) **1b**, (c) **1c**, and (d) **1d**: (—) predicted using the “sticky” dissociative ET model; (o) experimental through convolution analysis.

were calculated at the DFT/B3LYP/6-31G(p,d) level for different values of the S–Cl bond length.<sup>24</sup>

Figure 5 shows that for all studied compounds (**1a–d**), the obtained curves have the shape of Morse curves and show a clear energy minimum along the cleaved bond. Values of the bond lengths at the minimum energy ( $d_{\text{S-Cl}}$ ) as well as the interaction energies are reported in Table 6. This indicates that at least in the gas phase, strong interactions (0.277–0.383 eV) exist indeed between the generated fragments (radical/anion). An interesting result is that for all compounds **1a–d**, the minimum energies are observed at large distances (2.8–2.9 Å), suggesting the formation of radical/anion pairs rather than real radical anion intermediates. These distances are also in very good agreement with the ones determined from the earlier optimizations (Table 3). It is worth noting that the *p*-nitrophenyl sulfonyl chloride (**1d**) shows relatively higher interaction energy and that the maximum interaction is observed at a slightly shorter distance compared to compounds **1a–c**. This is in good agreement with what is expected, knowing that strong electron-withdrawing groups reinforce fragments clustering, as has been previously demonstrated.<sup>11</sup>

Figure 6 shows both the experimental as well as the predicted (using eq 3) activation free energy as a function of the driving force for the reduction of compounds **1a–d**. To obtain the best fit the interaction energy  $D_{\text{p}}$  has been adjusted. A very good fit is obtained for values of  $D_{\text{p}}$  lower than the ones estimated

**Table 6.** S-Cl Interaction Energy and Bond Length at the Minima

	<b>1a</b>	<b>1b</b>	<b>1c</b>	<b>1d</b>
$D_{\text{p}}^a$ (eV)	0.277	0.283	0.285	0.383
$D_{\text{p}}^b$ (eV)	0.020	0.020	0.020	0.150
$d_{\text{S-Cl}}$ (Å) <sup>c</sup>	2.9	2.9	2.9	2.8

<sup>a</sup> interaction energy calculated in gas phase. <sup>b</sup> interaction energy used for “sticky” dissociative ET model. <sup>c</sup> bond length at the minima in Å.

through gas-phase calculations (Table 6). This is expected since these interactions are smaller in solution owing to fragments solvation. It is worth noting that compound **1d**, with a strong electron-withdrawing group, shows a stronger interaction compared to compounds **1a–c**, as expected.<sup>11</sup> These data confirm the existence of radical/anion pair formation during the electrochemical reduction of *p*-substituted phenyl sulfonyl chlorides (**1a–d**). The dissociative ET to these compounds follows then a concerted mechanism, which leads the formation of a radical/anion cluster. As shown here and in full agreement of what has been reported in previous work,<sup>11–13</sup> such in-cage interaction, even if it is moderate in solution compared to gas phase, strongly affects the dynamics of the involved process. This is well observed here by an important decrease of the activation free energy of the electrochemical reduction of compounds **1a–d**.

Another consequence of the existence of such an interaction can be understood by comparing the standard reduction potentials to the reduction peak potentials for compounds **1a–d**. The difference between these two parameters (631 mV for **1a**, 558 mV for **1b**, 552 for **1c**, and 148 mV for **1d**) is lower than usually seen for classical concerted ET processes (more than 700 mV). In the particular case of compound **1d**, which shows the

(24) Optimization of the reduced forms of the studied structures (**1a–f** + one electron) at each bond length value at the B3LYP/6-31G(p,d) level has been performed using the Gaussian 2003 package.<sup>24b</sup> (b) Frisch, M. J.; et al. *Gaussian 03*; Gaussian, Inc.: Pittsburgh, PA, 2003.

strongest interaction between the *p*-nitrophenyl thiyl radical and the chloride anion, this difference is the smallest, showing that this compound is reduced near its standard reduction potential unlike what would have been observed without the involvement of such strong interactions.

## Conclusion

Important aspects of the electrochemical reduction of substituted arene sulfenyl chlorides were investigated. A striking change in the reductive cleavage mechanism as a function of the substituent and its position on the aryl ring of the arene sulfenyl chlorides is observed. With 2-nitrophenyl sulfenyl chloride (**1e**) and 2,4-dinitrophenyl sulfenyl chloride (**1f**) a stepwise ET mechanism is encountered where the electrochemical reduction leads to the intermediate formation of a radical anion (**1e,f**<sup>•−</sup>). A strong through space S<sup>•••</sup>O intermolecular interaction exists both at the level of the neutral molecules and at the radical anions as shown by the small distances between the two atoms at both stages. This interaction has a very important effect on both the dynamics and the nature of the initial ET mechanism for these two compounds (**1e,f**). Gas phase calculations support the electrochemical data, and minima for the reduced forms are obtained at relatively short S–Cl bond distances.

With para-substituted arene sulfenyl chlorides (**1a–d**), involving both electron-withdrawing and electron-donating groups (CH<sub>3</sub>, H, Cl, and NO<sub>2</sub>), a sticky dissociative ET takes place. The formation of a radical/anion pair is first suggested by the electrochemical data, which show that these compounds were easier to reduce than compounds **1e,f**. Further support for the existence of such in-cage interactions was provided by the gas phase calculations, which show substantial changes between the neutral structures and the minima obtained for their reduced forms, mainly an important elongation of the S–Cl bond (more than 0.7 Å).

Gas-phase potential energy profile curves of the reduced forms, of the studied compounds **1a–d**, along the cleaved S–Cl bond provided more insights into these radical/anion interactions in the gas phase and showed that, as expected, a strong electron-withdrawing substituent reinforces these interactions.

Applications of both classical and sticky dissociative ET models provided a final proof for the existence of fragments clustering during the electrochemical reduction of compounds **1a–d**. The fitting of the modeled and the experimental activation free energy–driving force curves allowed an estimation of the magnitude of these in-cage interactions in acetonitrile. The interactions are smaller compared to the gas phase and are more important for radicals bearing strong electron-withdrawing substituents. These interactions affect not only the activation free energy of the reaction but also its thermodynamics.

## Experimental Section

**Cyclic Voltammetry.** Electrochemical measurements were conducted in three electrode glass cells, thermostated at 25 °C, and under dry nitrogen. The working electrode is a 2 mm diameter glassy carbon electrode (Ekochemie). The electrode was carefully polished and ultrasonically rinsed with ethanol before each run. The reference electrode is SCE. The counter electrode was a platinum wire. The electrochemical instrument used is an Autolab PGSTAT30 especially configured to carry high scan rate CV experiments. A feedback correction was applied to minimize the Ohmic drop between the working and reference electrodes.

**Electrolyses.** The electrolyses were carried out in 20 cm<sup>3</sup> cells with a glassy carbon (Electrosynthesis) rectangular plate working electrode of 4 cm<sup>2</sup>. The counter electrode was a platinum grid, separated from the cathodic compartment by means of a glass frit. The reference electrode was the same as for CV. The cell was thermostated at 25 °C, and the solution was kept under a nitrogen stream during the whole electrolysis. The disappearance of the starting material and the formation of the products were followed by in situ cyclic voltammetry. The supporting electrolyte, tetramethylammonium tetrafluoroborate (TMAF), was extracted, and chromatographic analyses (HPLC and GCMS) were performed by comparison with authentic samples of the product.

**Chemicals.** Acetonitrile (Aldrich), the supporting electrolytes, tetramethylammonium tetrafluoroborate (TMAF), and TBAF (Fluka, puriss) were used as received.

4-Methylphenyl sulfenyl chloride (**1a**), phenyl sulfenyl chloride (**1b**), 4-chlorophenyl sulfenyl chloride (**1c**), 4-nitrophenyl sulfenyl chloride (**1d**), 2-nitrophenyl sulfenyl chloride (**1e**), and 2,4-dinitrophenyl sulfenyl chloride (**1f**) were prepared from either the corresponding thiol or disulfide or by reaction with sulfonyl chloride according to a well-known procedure.<sup>25</sup> All disulfides **2a–f** are commercially available (Aldrich) and were used as received.

**Theoretical Calculation.** The calculations were performed using the Gaussian 2003 package.<sup>24b</sup> LUMO orbitals were calculated after a full optimization without imposed symmetry of the conformations using the UHF, B3LYP method with the 6-31G+(d,p) basis set starting from preliminary optimizations performed with semiempirical methods. We checked that the obtained conformations were real minima by running frequency calculations for the UHF and B3LYP calculations. These calculations could not be performed at the MP2 level because of the too large molecule sizes.

**Acknowledgment.** We thank Dr. John D. Goddard for a series of instructive discussions concerning the theoretical calculations. A. Houmam gratefully acknowledges the Natural Sciences and Engineering Research Council (NSERC), The Canada Foundation for Innovation (CFI), the Ontario Innovation Trust (OIT), and the University of Guelph for funding.

**Supporting Information Available:** The theoretical calculation methodology and data of all studied compounds; complete ref 24b. This material is available free of charge via the Internet at <http://pubs.acs.org>.

JA062796T

(25) Harpp, D. N.; Friedlander, B. T.; Smith, R. A. *Synthesis* **1979**, 3, 181.